

Probing Current Sheet Instabilities from Flare Ribbon Dynamics

Ryan French (UCL MSSL), Sarah Matthews (UCL MSSL), Jonathan Rae (Northumbria University), Andrew Smith (UCL MSSL)



1. Introduction to Reconnection Instabilities

- In a solar flare, magnetic instabilities lead to the formation of a current sheet in which impulsive reconnection can take place. Insights into these current sheet dynamics can be probed by exploring flare ribbon substructure, as magnetic reconnection accelerates particles down reconnected field lines to the chromosphere to mark the flare footpoints. Footpoint behaviour can therefore provide insights into processes within the current sheet.
- There are several key candidates for the dominant instability in flares (e.g. tearing mode or Kelvin-Helmholtz), each with characteristic growth rates and spatial/temporal scales predicted by theory.
- Motivated by a similar study on the Earth's magnetosphere (*Kalmoni et al 2015, 2018*) and the work by *Brannon et al (2015)*, we search for key spatial scales in the fluctuating ribbon intensities, with the aim of exploiting their magnetic connectivity to the current sheet and explore instability properties at the reconnection site.
- To complete this work, we will compare these observed scales with those predicted by theory for different theoretical instabilities.

2. Small B-class flare on December 6th 2016

- The small flare was observed by IRIS SJI 1400 Å with a high cadence of 1.7 s. The slit passes through the east ribbon (*Jeffrey et al 2018*), but here we focus on the spatial and temporal evolution of the ribbon intensity structure.
- The light curve in Fig 1 shows both ribbons brightening cotemporally. Peak ribbon intensity is followed by the appearance of emission in AIA 131, as heated material from the chromosphere fill the loops.

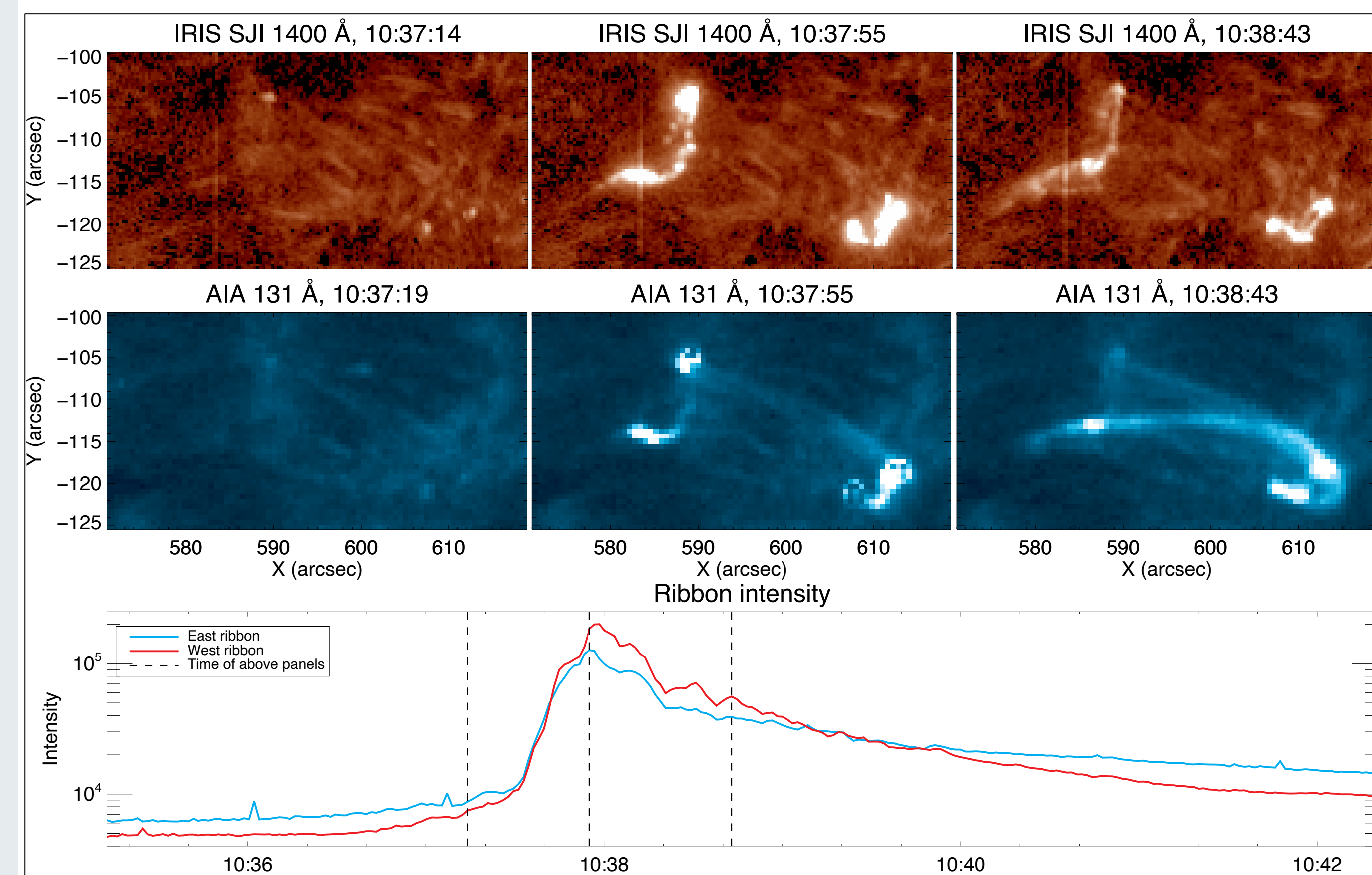


Fig 1: Top: Evolution of IRIS SJI 1400 Å. Middle: Evolution of AIA 131 Å. Bottom: Ribbon light curve, of masked region in Fig 2.

3. Flare Ribbon Tracking

- We track a central slit along the evolving ribbons, plotting the mean intensity around each pixel along the slit (Fig 2).
- Next, we detrend the intensity cross-section, apply a Hanning Window, and calculate the spatial Fast-Fourier Transform for each time step.

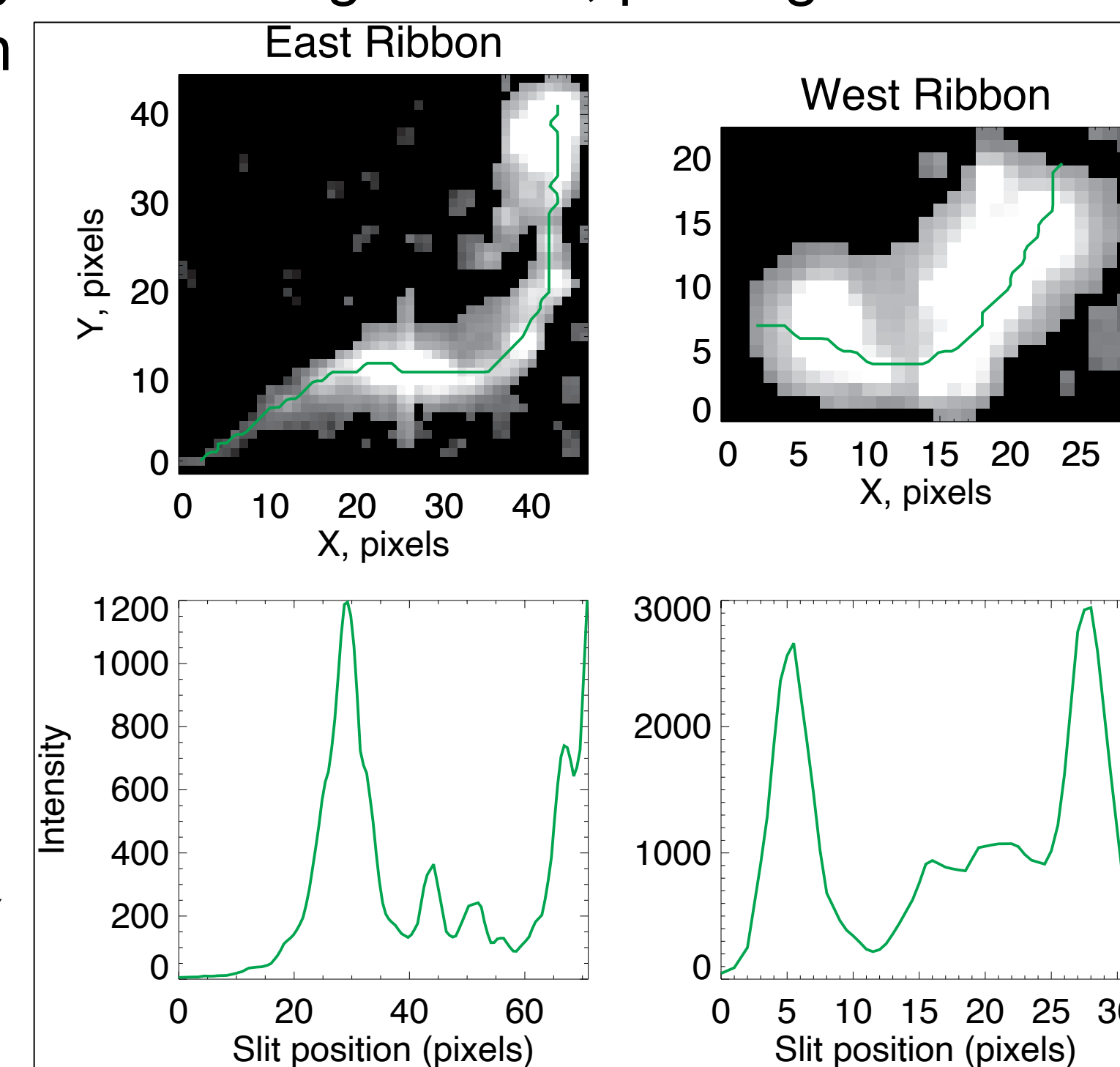


Fig 2: Top: 10:37:55 UT snapshot of the ribbon centroid-tracking slit, along the masked data. Bottom: Intensity cross-section along the slit in top panel.

4. Power and Intensity Evolution

- Examining the intensity and power stack plots below, we detect a spatial periodicity in the ribbon bright regions in the minutes leading up to the flare impulsive phase. This occurs at a scale of 8&14 in the west ribbon, and 11& (potentially) 23 pixel widths at the east.
- This is followed by exponential growth at certain wavelengths, marked by the vertical dashed lines and explored further in Fig 5.

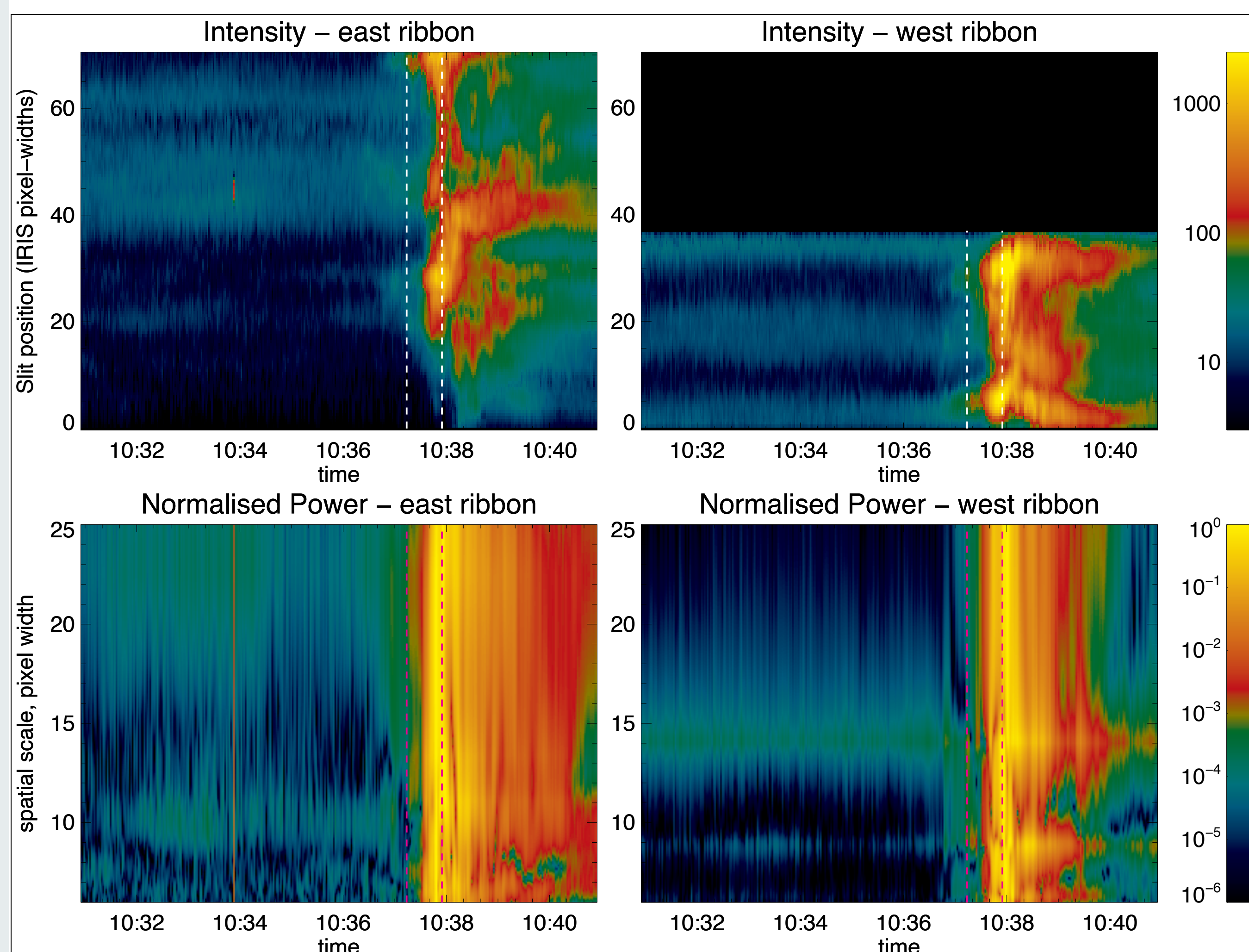


Fig 3: Top: Ribbon intensity stack plots. Bottom: Wavelength power stack plots, normalised at each wavelength. All y-axes in units of IRIS pixel-width (0.33 arcsec). Dashed lines mark period of exponential power growth.

5. Exponential Growth in Power Spectra

- Examining cross-sections through the power data (Fig 4, top), we determine the rate and period of exponential growth at each wavelength. This exponential growth at the majority of spatial scales is a classical indication of plasma instabilities.
- Fitting the exponential phase provides the variation in growth rate / duration with wavelength at each flare footpoint.
- Examining photospheric flux, we find BxArea is equal in both ribbons, implying flux conservation between the connected ribbons. We use the ribbon area relationship to scale the west ribbon wavelengths to the spatial frame of the east ribbon (Fig 4). This allows us to verify observed scales in each ribbon are connected by a common process (most likely, dynamics in the current sheet).
- Fig 4 shows the growth rate at each ribbon, starting at a spatial scale of 7.3 pixel widths.

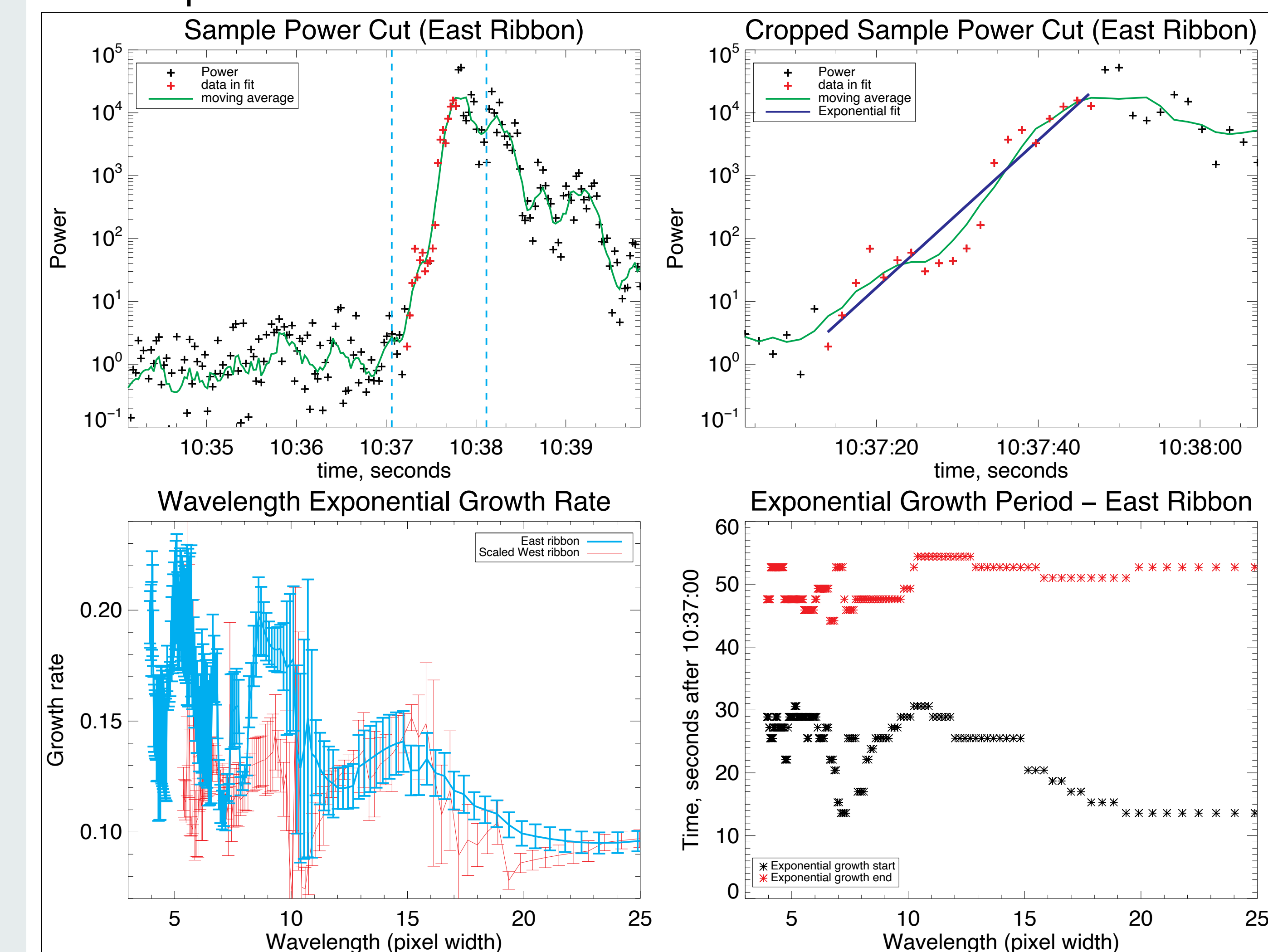


Fig 4: Top: Cross-section through power plot (Fig 3) at wavelength=7.33 pixel widths, showing exponential growth. Bottom left: Exponential growth rate at each wavelength. West scales are transformed to east scales. Bottom right: Start/end times of the fitted exponential period.

6. Summary

- We detect exponential growth across most spatial scales in the two ribbons of a small, simple flare, with key wavelengths aligning when scaled. This is a classic indicator of reconnection instabilities.
- Next, we will compare observed scales and growth-rates with predictions by theory/simulations for different instabilities, to determine the dominant trigger processes in this flare case-study.